Int J Thermophys (2008) 29:1084–1093
DOI 10.1007/s10765-008-0387-z

Filter Radiometers as a Tool for Quality Assurance of Temperature Measurements with Linear Pyrometers

M. Ojanen · V. Ahtee · M. Noorma · T. Weckström · P. Kärhä · E. Ikonen

Published online: 29 February 2008

Abstract Measurements made with a pyrometer are vulnerable to errors if the pyrometer is misaligned, inaccurately characterized, or malfunctioning. In this work, thermodynamic temperatures between 1,373 and 1,773 K were studied by measuring a variable-temperature blackbody with a linear pyrometer and four absolutely characterized filter radiometers. The filter radiometer measurements were done in the irradiance mode. In the first set of measurements, there was a 3–5 K difference between the pyrometer and the filter radiometer data. The cause was tracked to malfunctioning of the pyrometer, which was afterwards sent for repair on the basis of these results. In the second set of measurements, with the repaired pyrometer, the agreement of the temperature results was good, the mean difference being −0.41 K with a standard deviation of 0.52 K. The differences between the pyrometer and the filter radiometer temperature measurement results showed no temperature dependence. It was concluded that the filter radiometers used in the irradiance mode provided a straightforward method for the quality assurance of pyrometers.

Keywords Filter radiometer · Fixed-point cell · Quality assurance · Variable-temperature blackbody

M. Ojanen (✉) · V. Ahtee · M. Noorma · P. Kärhä · E. Ikonen
Metrology Research Institute, Helsinki University of Technology (TKK), Espoo, Finland
e-mail: maija.ojanen@tkk.fi

V. Ahtee · T. Weckström · E. Ikonen
Centre for Metrology and Accreditation (MIKES), Espoo, Finland

Present Address:
M. Noorma
Tartu University, Tartu, Estonia

1 Introduction

Above the freezing temperature of silver (Ag), 1,234.93 K, the International Temperature Scale of 1990 (ITS-90) is based on Planck's radiation law and reference temperatures defined by phase transition temperatures of metals. These auxiliary temperatures are realized with fixed-point cells. The thermodynamic temperature of an object can be derived from the measured spectral irradiance. Above 1,357.77 K (Cu point), the measurements are purely extrapolated [1].

The extrapolated temperature measurements can be carried out using a pyrometer. Such measurements are vulnerable to errors if the pyrometer is misaligned, inaccurately characterized, or malfunctioning. The causes for malfunction can be characterization inaccuracies of the pyrometer components, or broken components, for example, in the electronics part. The problems may manifest themselves as nonlinearity, drift of the results, or instability of the calibration. Thus, the quality of the measurements should be assured by some means.

Assessment of the extrapolated pyrometer measurements can be made using eutectic fixed-point cells. However, these devices are not yet widely available to most calibration laboratories. Assessment can also be done using detector-based methods. Temperatures of a variable-temperature blackbody radiator can be measured with absolutely characterized filter radiometers, and the extrapolation of the pyrometer can be verified with these measured temperatures. Several different absolute methods for the radiometric temperature measurements have been studied and compared with the ITS-90 based realizations [2–4]. In these methods, the spectral radiance of a blackbody source is either measured directly, or it is calculated from the spectral irradiance measured at a known distance from the source. Several intercomparisons have shown improvement of the agreement among different national metrology institutes in the temperature range between 1,570 and 3,270 K [5–7]. In our previous study, the freezing temperature of a copper fixed-point cell was measured at three different wavelengths and found to be in good agreement with ITS-90 [8].

In this work, thermodynamic temperatures between 1,373 and 1,773 K were studied by measuring a variable-temperature blackbody. The measurements were carried out using a linear pyrometer and four absolutely characterized filter radiometers with effective wavelengths between 600 and 900 nm. The filter radiometer measurements were done in the irradiance mode. The results obtained with the pyrometer and the filter radiometers were compared. Prior to the variable-temperature blackbody measurements, the absolutely characterized filter radiometers were tested on a silver fixed-point cell for which the freezing temperature is 1,234.93 K. The same cell was used to calibrate the linear pyrometer. Two sets of measurements were made in 2004 and 2006. The results of the first measurements indicated severe malfunctioning of the pyrometer, and it was sent for repair. After the repair, the repeated measurements showed significantly better agreement.

In Sect. 2, the theory of the radiometric temperature measurements is introduced. The components used, including the linear pyrometer, the filter radiometers, the blackbody, and the fixed-point cells, are described. An uncertainty analysis is presented for the filter radiometer measurements. In Sect. 3, the measurement results obtained in 2004 and 2006 are presented and compared. The conclusions are presented in Sect. 4.

2 Materials and Methods

2.1 Radiometric Temperature Measurements

The thermodynamic temperature of a blackbody source can be determined from the measured spectral irradiance at a known distance. The measurement setup is illustrated in Fig. 1. The radiant flux of the blackbody is measured using a filter radiometer, which converts the received optical power into a photocurrent. The relation between the photocurrent i and the thermodynamic temperature T is determined by

$$i = \frac{A_{\mathrm{BB}}\left(1+\frac{r_{\mathrm{BB}}^2 r_{\mathrm{FR}}^2}{D^4}\right)}{D^2}\varepsilon \int S(\lambda)\, L(\lambda, T)\, \mathrm{d}\lambda, \tag{1}$$

where λ is the wavelength and $S(\lambda)$ is the spectral irradiance responsivity of the filter radiometer calculated from the filter transmittance, the detector responsivity, and the aperture area of the filter radiometer. The function $L(\lambda, T)$ is the spectral radiance of the blackbody output given by Planck's radiation law, A_{BB} is the aperture area of the blackbody, r_{BB} is the radius of the blackbody aperture, r_{FR} is the radius of the filter radiometer aperture, and ε is the emissivity of the blackbody . The geometric factor D is defined by $D^2 = d^2 + r_{\mathrm{BB}}^2 + r_{\mathrm{FR}}^2$, where d is the distance from the filter radiometer aperture to the blackbody aperture.

The theoretical current is calculated using Eq. 1. The current from the filter radiometer is converted into a voltage and measured using a current-to-voltage converter and a digital multimeter. At first, the temperature is set to the initialization value, e.g., the pyrometer reading. Then, the difference between the theoretical and measured currents is minimized by adjusting iteratively the temperature used in Eq. 1.

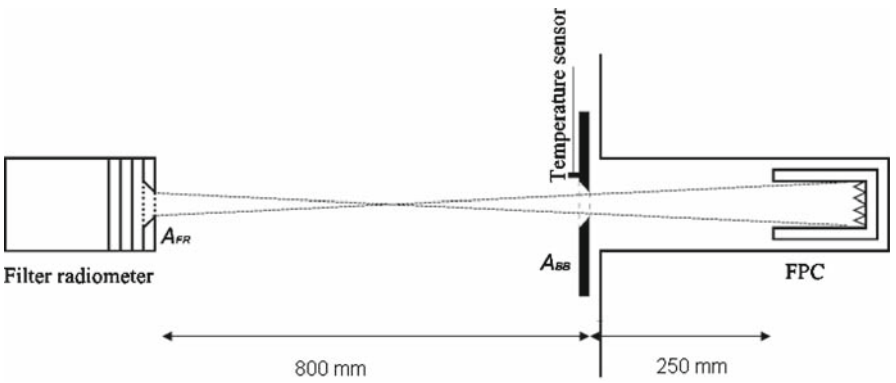

Fig. 1 Setup used for fixed-point cell (FPC) and variable-temperature blackbody (VTBB) measurements. A_{FR} is the filter radiometer aperture area, and A_{BB} is the defining area for the blackbody

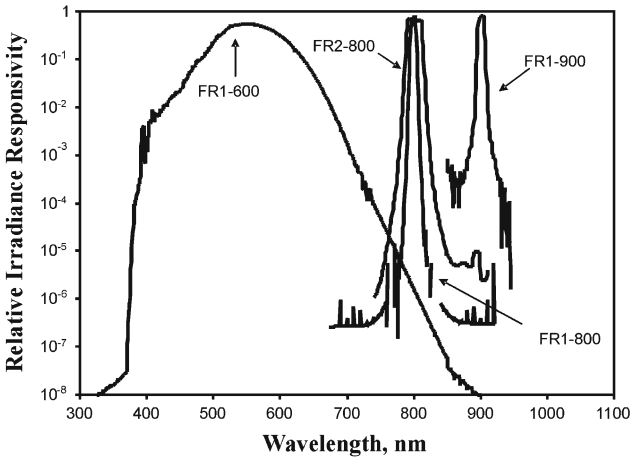

Fig. 2 Spectral responsivities of the filter radiometers

2.2 Filter Radiometers

Reference [9] gives a detailed description of the filter radiometers. They consist of a trap detector made of three silicon photodiodes, a precision aperture, and a bandpass filter. Two separate filter radiometer constructions, FR1 and FR2, were used. The FR1 radiometer had an interchangeable filter, the housing being the same for each of them. Its components were characterized separately, as described in [10]. FR1-600 had a broadband $V(\lambda)$-filter with an effective wavelength of 603 nm. The other filters had effective wavelengths of 800 and 900 nm and narrow pass-bands of 10 nm. The spectral irradiance responsivities of the filter radiometers are shown in Fig. 2.

The structure of FR2-800 includes a permanently installed filter with a central wavelength of 800 nm and a bandwidth of 20 nm. The FR2-800 radiometer was characterized as a whole package with the help of a wavelength-tunable Ti:sapphire laser. The characterization method is described in more detail in [11].

2.3 Linear Pyrometer

The linear pyrometer used in our study has a measurement range from 1,000 to 2,800 K and a valid calibration from 1,200 to 1,800 K. The temperature T_{LP} is calculated using the Sakuma-Hattori equation,

$$T_{\mathrm{LP}} = -\frac{c_2}{a\ln\left(I_{\mathrm{ph},\lambda}/\mathrm{c}\right)} - \frac{b}{a}, \tag{2}$$

where $I_{\mathrm{ph},\lambda}$ is the measured photocurrent, $c_2 = 1.4488 \times 10^{-2}\,\mathrm{K\cdot m}$ is the second radiation constant, and constants $a = 641.09 \times 10^{-9}\,\mathrm{m}$, $b = 10.07 \times 10^{-6}\,\mathrm{K\cdot m}$, and $c = 715.0 \times 10^{-6}\,\mathrm{A}$ are determined by calibration.

2.4 Measurement Setup

An Ag fixed-point cell (FPC) and a variable-temperature blackbody (VTBB) were used as blackbody sources. The inner length of the cavity of the Ag FPC was 50 mm and the inner diameter of the cavity was 10 mm. The crucible of the FPC is made of Ultra Carbon Grade UT-6ST graphite. The back wall of the cavity has a periodic structure of little cones approximately 5 mm height to increase the emissivity.

The emissivity of the FPC was calculated based on the material emissivity, the shape of the cavity, and the temperature distribution using STEEP3 software [12]. The emissivity was found to be 0.9980 ± 0.0002 in the wavelength range between 600 and 900 nm.

The measurement setup is described in Fig. 1. The FPC was mounted inside an electrically heated horizontal-tube furnace. A defining aperture of aluminum was placed in front of the furnace. The distance from the detector to the defining aperture of the blackbody was measured using an optical rail with a magnetic distance measurement unit. During these measurements, the distance between the detector aperture and the defining aperture of the blackbody was kept at 800 mm. The diameters of the defining aperture and the detector aperture were both 3.4 mm. The aperture areas were measured using a laser scanning technique [13].

The temperature of the defining aperture was kept constant at 40°C with a thermoelectric temperature controller. In addition, the temperature was monitored continuously with a thermistor, which was glued to the aperture. During the measurements of higher temperatures (1,373–1,773 K), the aperture temperature increased despite the cooling. The thermal expansion of the aperture was taken into account in the calculation of the area of the defining aperture by using the thermal expansion coefficient of aluminum, $2.32 \times 10^{-5}\,\mathrm{K}^{-1}$. The typical temperature noted at 1,773 K for the aperture was 50.0°C, resulting in a correction of 0.1% in the aperture area. The entrance aperture of the filter radiometer was aligned with the optical axis defined by the center of the defining aperture and the center of the FPC. The alignment was made using a dual-beam alignment laser. The measurement geometry was chosen so that the filter radiometer received a signal coming from the back wall of the FPC.

A correction factor to compensate the diffraction losses was calculated using diffraction software [14]. The calculation is based on the measurement geometry. The diffraction corrections were found to be 0.9975, 0.9966, and 0.9962 for filter radiometers FR1-600, FR1-800, and FR1-900, respectively. The diffraction correction for FR2-800 is 0.9966, the same as for FR1-800.

Before the measurements, the melting and freezing temperature of the FPC was monitored with the linear pyrometer. The freezing temperature was then measured with the filter radiometers. After the measurements, the temperature was re-checked with the pyrometer. The total duration of a single set of measurements was approximately 1.5 h.

The VTBB temperature measurements were made using a similar setup and method as for the FPC measurements. The VTBB has a cylindrical graphite cavity with an inner diameter of 110 mm and a length of 232 mm. The cavity has a 15 mm diameter aperture and a conical back wall. The emissivity was calculated to be 0.9998 ± 0.0002 at all wavelengths and temperatures used. The diffraction losses were considered

Table 1 Uncertainties of the temperature measurements with the filter radiometers at 1,234.93 K

Component	FR1-600	Contribution to uncertainty (K)		
		FR1-800	FR1-900	FR2-800
Area of filter radiometer aperture	0.019	0.026	0.029	–
Area of blackbody aperture	0.025	0.034	0.037	0.035
Wavelength	0.094	0.061	0.050	0.005
Filter transmittance	0.069	0.092	0.105	–
Power responsivity of trap detector	0.026	0.048	0.067	–
Spectral irradiance responsivity	–	–	–	0.088
Distance	0.019	0.026	0.029	0.026
Current measurement	0.292	0.015	0.008	0.010
Diffraction	0.005	0.005	0.005	0.005
Emissivity	0.031	0.041	0.047	0.041
Out-of-band leakage	0.008	0.020	0.024	0.010
Combined standard uncertainty, $k = 1$	0.319	0.139	0.155	0.107
Expanded uncertainty, $k = 2$	0.638	0.278	0.309	0.215

negligible. With the VTBB, the radiating bottom of the cavity is closer to the limiting aperture that reduces diffraction as compared to the geometry with the FPC.

2.5 Measurement Uncertainties

2.5.1 Filter Radiometers

The uncertainty components of the filter radiometers and their contribution to the total uncertainty are presented in Table 1. The filter transmittances were measured with an uncertainty of 0.09% using a double-beam transfer standard spectrometer whose performance was checked against a reference spectrometer. The power responsivity determination of the trap detector was done by a laser calibration: the responsivity was measured at four different laser wavelengths, and a responsivity model was used to extend the calibration over the whole wavelength range. FR2-800 was calibrated using a wavelength-tunable laser [11], which results in somewhat lower wavelength and responsivity uncertainties than those of the other filter radiometers. The uncertainty of the responsivity model is between 0.06% and 0.365%, depending on the wavelength. For the FR1 filter radiometers, the largest uncertainty components arise from the wavelength calibration, the filter transmittances, and the power responsivity of the trap detector. The current measurement uncertainty of the FR1-600 results from a lower signal level, which causes a relatively higher dark current contribution.

The uncertainty of the distance measurement was 0.1 mm. Distances were measured using a magnetic rail with a distance measurement unit. The method for the calibration of the current-to-voltage converters is described in [15]. The uncertainty is

wavelength dependent, as the spectral radiance varies with wavelength. The relation between current and radiance is given in Eq. 1. The diffraction losses and the emissivities of the sources were calculated as discussed in Sect. 2.4. The uncertainties of these components arise from the uncertainties of the models used, the distance determination, and the aperture-area measurements. The uncertainties caused by out-of-band leakages were estimated by comparing the anticipated out-of-band signal with the pass-band signal. The combined standard uncertainties at 1,234.93 K are 0.319, 0.139, 0.155, and 0.107 K for the filter radiometers FR1-600, FR1-800, FR1-900, and FR2-800, respectively.

2.5.2 Linear Pyrometer

The linear pyrometer was calibrated in 2005 for the range from 1,200 to 1,800 K by the manufacturer after it was rebuilt. The overall uncertainty is 0.75 K ($k = 1$) for the temperature measurements within the measurement range of this study. The uncertainties of the pyrometer measurement arise from the filter transmittances, the reflectance of the pyrometer optics, and the responsivity of the detector.

3 Measurement Results

3.1 Fixed-Point Cell Measurements

In 2006, the filter radiometers were first tested on a silver FPC. The measurements were repeated three times. Figure 3 presents the average results and their deviations from the ITS-90 value. The deviations from the ITS-90 value were 0.19 K for FR1-600, 0.74 K for FR1-800, 0.27 K for FR1-900, and −0.06 K for FR2-800. Excluding the measurement with filter radiometer FR1-800, the measurement results are within the expanded uncertainty limits presented in Table 1.

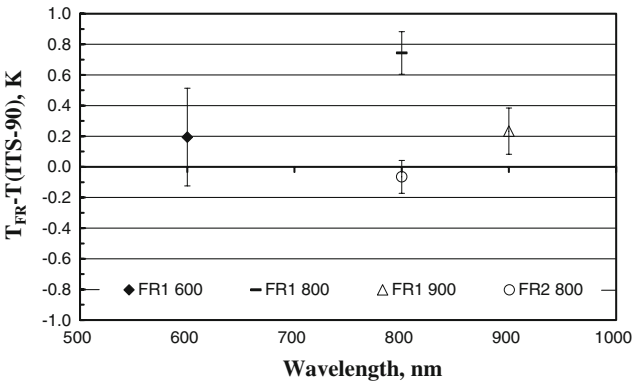

Fig. 3 Fixed-point cell measurement results. The vertical axis is the difference between the measured and ITS-90 temperatures. Standard uncertainties are given with a coverage factor of $k = 1$

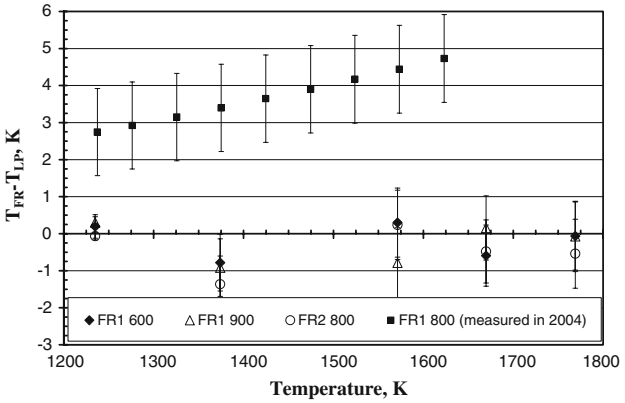

Fig. 4 Differences of the variable-temperature blackbody temperatures measured with a filter radiometer and the pyrometer in 2004 and in 2006. For the 2006 measurements, filled diamonds, open triangles, and open circles correspond to FR1-600, FR1-900, and FR2-800 data, respectively. Standard uncertainties ($k = 1$) associated with the comparison of the filter radiometer and pyrometer are indicated

3.2 Variable-Temperature Blackbody Measurements

3.2.1 Measurements in 2004

The first set of measurements from 2004 shows a clear difference between the pyrometer and the filter radiometer FR1-800 measurement data, as can be seen in the upper set of data in Fig. 4. The deviations increase linearly with temperature. The deviations exceed 2.5 K, and the maximum deviation is 4.7 K at 1,623 K. The cause of the deviation was tracked to malfunctioning of the pyrometer, which was then sent for repair. The increasing deviation of the results with temperature may indicate problems with the optics. The properties of the filter (e.g., the effective wavelength) may have changed after the calibration. Another possibility for the deviation is the nonlinearity of the detector or the electronics, which may be due to failure of certain components or their overheating. We also observed instability of the pyrometer readings; the fixed-point calibration could change when measuring on consecutive days.

3.2.2 Measurements in 2006

In 2006, the variable-temperature blackbody measurements were repeated after the pyrometer was returned from repair. The results are presented as the lower set of data in Fig. 4 for the filter radiometers FR1-600, FR1-900, and FR2-800. The deviation between the pyrometer and the filter radiometers is significantly reduced compared to the results from 2004. The mean of the differences is −0.41 K and the standard deviation is 0.52 K. The uncertainty bars correspond to the quadratic sum of the uncertainties of the pyrometer and the filter radiometers. The uncertainty components of the filter-radiometer measurements are similar to those in Table 1. In addition, the uncertainties caused by the thermal expansion of the defining aperture

(from 0.006 to 0.015 K) and the temperature drift of the furnace have been added. The drift was accounted for by measuring with the pyrometer before and after the filter-radiometer measurements and using the average of the measurements for the comparison. The drift was found to be quite linear, and most of it could be compensated afterwards. The standard uncertainties due to the drift and fluctuations are 0.04, 0.52, 0.33, and 0.49 K for the temperatures 1,373, 1,573, 1,673, and 1,773 K, respectively, calculated as the differences of the maximum and minimum values divided by $2\sqrt{3}$.

4 Conclusions

The thermodynamic temperatures of a silver fixed-point cell and a variable-temperature blackbody were measured using four filter radiometers at different wavelengths and a linear pyrometer. The results were compared in order to assure the quality of the pyrometer measurement results. In addition, the reliability of the filter-radiometer results also benefits from a comparison against other filter radiometers or fixed-point cells.

During the first measurements, there was a large difference between the pyrometer and the filter-radiometer measurement results. At low temperatures near the calibration point, there was good agreement, but at high temperatures, the deviation increased as a function of temperature. The pyrometer measurements were also unstable. After the pyrometer was repaired, the agreement with the filter-radiometer results was good, the mean difference being −0.41 K and the standard deviation 0.52 K. The difference between the pyrometer and the filter radiometers showed no temperature dependence. The results were also repeatable on consecutive measurement days, which showed that the instability of the calibration had been resolved. The uncertainties are due to the temperature fluctuation of the furnace and the calibration uncertainties of the different components of the measurement setup.

The malfunction could not have been detected using conventional fixed-point cells. We conclude that the relative measurements with pyrometers need quality assurance. In these devices, there are fault mechanisms (e.g., changes in optics or the detector following calibration) that may cause errors in the extrapolation. The faulty measurements cannot necessarily be seen in the calibrations with only one fixed-point cell, but they are revealed if a eutectic cell or VTBB with filter radiometers is used. On the other hand, the instability problems with the electronics of the pyrometer can be revealed by fixed-point calibrations. The fixed points provide a stable calibration source against which the fluctuation of the pyrometer reading can be easily observed. For other types of malfunctioning of the pyrometer, VTBB and filter radiometers used in the irradiance mode provide a straightforward method to obtain the required quality assurance. The pyrometer is still a suitable instrument for everyday use, as the measurements can be done directly in the radiance mode without the need for defining apertures.

Acknowledgment The corresponding author, Maija Ojanen, acknowledges the support from Tekniikan Edistämissäätiö (Finnish Foundation for Promoting Technology).

References

1. H. Preston-Thomas, Metrologia **27**, 3 (1990)
2. N. Fox, J.E. Martin, D.H. Nettleton, Metrologia **28**, 357 (1991)
3. H.W. Yoon, C.E. Gibson, P.Y. Barnes, Appl. Optics **41**, 5897 (2002)
4. M. Stock, J. Fischer, R. Friedrich, H.J. Jung, R. Thornagel, G. Ulm, B.Wende, Metrologia **30**, 439 (1993)
5. N.J. Harrison, N.P. Fox, P. Sperfeld, J. Metzdorf, B.B. Khelynov, R.I. Stolyarevskaya, V.B. Khromchenko, S.N. Mekhontsev, V.I. Shapoval, M.F. Zelener, V.I. Sapritsky, Metrologia **35**, 283 (1998)
6. H.W. Yoon, P. Sperfeld, S. Galal Yousef, J. Metzdorf, Metrologia **37**, 377 (2000)
7. B.B. Khelvnoy, N.J. Harrison, L.J. Rogers, D.F. Pollard, N.P. Fox, P. Sperfeld, J. Fischer, R. Friedrich, J. Metzdorf, J. Seidel , M.L. Samoylov, R.I. Stolyarevskaya, V.B. Khromchenko, S.A. Ogarev, V.I. Sapritsky, Metrologia **40**, S39 (2003)
8. M. Noorma, P. Kärhä, T. Jankowski, F. Manoocheri, T. Weckström, L. Uusipaikka, E. Ikonen, in *Proceedings of TEMPMEKO 2004, 9th International Symposium on Temperature and Thermal Measurements in Industry and Science*, ed. by D. Zvizdić, L.G. Bermanec, T. Veliki, T. Stašić (FSB/LPM, Zagreb, Croatia, 2004), pp. 101–106
9. P. Kärhä, A. Haapalinna, P. Toivanen, F. Manoochehri, E. Ikonen, Metrologia **35**, 255 (1998)
10. P. Kärhä, P. Toivanen, F. Manoocheri, E. Ikonen, Appl. Optics **36**, 8909 (1997)
11. M. Noorma, P. Toivanen, F. Manoocheri, E. Ikonen, Metrologia **40**, 220 (2003)
12. A.V. Prokhorov, Metrologia **35**, 465 (1998)
13. A. Lassila, P. Toivanen, E. Ikonen, Meas. Sci. Technol. **8**, 973 (1997)
14. K.D. Mielentz, J. Res. Natl. Inst. Stand. Technol. **103**, 497 (1998)
15. P. Sipilä, R. Rajala, P. Kärhä, A. Manninen, E. Ikonen, *Proceedings of NEWRAD 2005, International Conference on New Developments and Applications in Optical Radiometry*, ed. by J. Gröbner (WRC/PMOD, Davos, Switzerland, 2005), pp. 223–224